

## Operational of Canny Algorithm on SAR data for modelling shoreline change

MAGED MARGHANY, Kuala Terengganu/Malaysia

**Abstract:** This study introduces a new approach for operational of SAR polarized data on coastal erosion studies. Polarized TOPSAR and ERS-1 data are used for this purpose. ERS-1 data was acquired on the 8<sup>th</sup> August 1993 and polarized TOPSAR data was acquired on the 6<sup>th</sup> December 1996. A quasi-linear model and a new model based on the Canny algorithm were used to model shoreline changes. Digitized vector layers of shoreline change were used to examine the accuracy of the model results. This study shows that the results of the Canny algorithm has a good correlation with the results from the quasi-linear model. The Canny algorithm can successfully be used for automatic detection of shoreline change. In conclusion, the integration between the quasi-linear model and the Canny algorithm model enables further operational of SAR data for coastal erosion studies.

**Zusammenfassung:** Zur Anwendung des Canny Algorithmus auf SAR-Daten für die Modellierung der Änderungen von Uferlinien. In dieser Studie wird eine neue Methode zur operationellen Anwendung von polarisierten SAR-Daten zur Erfassung von Küstenerosionen vorgestellt. Für diesen Zweck werden ERS-1- und multipolarisierte TOPSAR-Daten verwendet. Die ERS-1-Daten wurden am 8. August 1993 und die polarisierten TOPSAR-Daten am 6. Dezember 1996 gewonnen. Zur Modellierung der Veränderungen der Küstenlinie wurde ein quasi-lineares Modell verwendet und ein daraus abgeleitetes neues Modell, basierend auf dem Canny Algorithmus. Zur Überprüfung der Genauigkeit der Modellierungsergebnisse sind digitalisierte Vektordarstellungen der Veränderungen der Küstenlinien angefertigt worden. Die Studie ergab eine gute Korrelation der Ergebnisse des Canny-Algorithmus mit denen des quasi-linearen Modells. Der Canny Algorithmus kann erfolgreich zur automatischen Bestimmung von Veränderungen der Küstenlinie angewendet werden. Zusammenfassend kann festgestellt werden, dass die Integration von quasi-linearen Modellen mit Canny-Algorithmus-Modellen die Möglichkeiten zur Anwendung von SAR-Daten für Studien zur Küstenerosion erweitert.

### 1 Introduction

Operational of synthetic Aperture Radar (SAR) on coastal erosion studies has not established yet. In the fact that scientists are focusing in SAR wave model evaluation. The operational of SAR data on coastal erosion should be considered. The operational of SAR data on coastal erosion is required standardized procedures. The procedures should be involved a number of models. These models will be able to operate the SAR data on coastal erosion studies. The operational model will induce high rates of

accuracy compared to classical methods. The classical methods of coastal erosion studies which restricted with digitizing and overlaying techniques provided high rate of errors. There are several problems derived from classical methods. These methods provide high rates of error and require a lot of time to process the data. In this process, the sum of thematic errors and digitizing errors account for low accuracy of the interpretation results. Furthermore these methods are not able to recognize the dynamics interaction of waves energy and sediment transport. These often results in adequate solu-

tions of the problems for coastal engineers and decision makers. For instance, RAJ (1982), MAZLAN et al. (1989), and FRIGHY et al. (1994) used different historical data of satellite imagery, aerial photography and topographic maps for coastal erosion studies. Most of these studies found an unrealistic high rate of erosion of more than 50 m/year. For instance, FRIGHY et al. (1995) found the rate of erosion in the Nile Delta to be  $-70.8$  m/year. However, if this rate really had occurred, it would have caused the destruction of all the infrastructures, such as roads and bridges near the coastal waters. Furthermore, FRIGHY et al. (1995) stated that there is a significant relation between shoreline change, estimated from Landsat TM, aerial photography and ground surveys with a correlation coefficient ( $r$ ) of 0.93. This can not be considered as a significant result, due to the fact that a significant statistical test such as ANOVA or the t-test have not been performed. In addition, the low resolution of the Landsat data (30 m) only justifies its use in coastal erosion studies with changes that are larger than this pixel size. As a matter of fact, the resolution of this sensor is unable to capture beach profiles at a width less than the pixel size ( $< 30$  m). The high resolution of SPOT PAN (10 m) and radar data such as from ERS-1 (12.5 m), RADARSAT (12.5 m) and AIRSAR/TOPSAR (ca. 10 m) enables us to solve this type of problem.

The obvious critical problem was in coastal erosion studies from space is misunderstanding of the nature of sediment transport. It was reasonable in the study of EL-RAEY et al. (1995). They reported that the sea level rise along the Rossate (branch of the Nile river delta, Egypt) is main factor in causing coastal erosion. However, FRIGHY et al. (1995) have concluded that the erosion along Rossate is due to the effect of Aswan High Dam. The contrast between studies is indicating misunderstanding to the nature of the problem. The energy of the river flood was acting as nature coastal defence. The high energy of river flood just reduced the wave energy input in nearshore. After the High Dam built, this phenomena

has not been occurred. Then, the wave energy can easily induced high rate of erosion.

Recently, MAGED (1999) introduced a new approach for coastal erosion studies. A radon transformation was used to detect shoreline changes. MAGED compared the results of radon transformation with the results of classical methods of shoreline identification by the digitizing and overlaying method. He found that the error is significantly lower while using the radon transformation. However, radon transformation can not be applied to concave shorelines since it can only deal with linear features in the images. MAGED's study (1999) could not fully explain this type of shoreline change as it appeared to be concave in some places. So the conclusion might be that radon transformation is not suitable to apply to these non-linear features but only to straight shorelines.

The operational models could be new method for coastal erosion detection. This method will be useful for rapid detection and illustrative for educational purposes. In order to make the coastal erosion model operational, the integration between wave spectra effects and automatic detection of shoreline (over time and space) should be recognized. The aim of this study is to introduce a new approach for operational use of polarized SAR data in coastal erosion studies.

## 2 Methodology

### 2.1 Study Area

The study area is located in the South China Sea between  $5^{\circ} 21' N$  to  $5^{\circ} 27' N$  and  $103^{\circ} 10' E$  to  $103^{\circ} 15' E$ . This area lies in the equatorial region and is dominated by two monsoon seasons (MAGED 1994). The southwest monsoon lasts from May to September while the northeast monsoon lasts from October to March. The monsoon winds effect the direction and magnitude of waves. Strong waves with maximum height of 4 m are prevalent during the northeast monsoon when prevailing wave direction is from the north (December to February), while during

the southwest monsoon (May to September), the wave direction is from the south (MAGED 1999) with wave height less than 1 m.

**2.2 Data Acquired**

SAR data used in this study included ERS-1 and AIRSAR/TOPSAR data. ERS-1 data in the Cvv band (12.5 m) was acquired on 8<sup>th</sup> August 1993. AIRSAR/TOPSAR data with composite polarization in the L band (HH and VV polarization) with 10 m pixel resolution was acquired on 6<sup>th</sup> December 1996.

**2.3 Shoreline Change Model**

The shoreline change model utilizes shoreline definition, speckles reduce, canny algorithm, wave spectra detection and final shoreline change model based on the rate change of volume of sediment transport (Fig. 1).

In ease of shoreline detection, the shoreline of the East Coast of the Peninsula of Malaysia is defined by the boundary between the vegetation and the bare sandy area (beach) (MAGED 2000). This definition will be more useful in determining the shoreline from polarized SAR data. It is well known that SAR data contain speckled noise which induces limitation on the visual interpretation of SAR images. Linear filters, such as Gaussian filtering and Lee filtering could be applied to enhance the image for visual interpretation. The Canny algorithm has been implemented for shoreline detection. It provides a way of edge detection of the shoreline, as close as possible to the true edges. This has been examined by manual digitizing and overlaying of shoreline maps derived from the radar imagery. The Canny filtering algorithm was applied as follows:

The input of the image intensity is  $I$ , which is corrupted by noise. Let  $G$  be a Gaussian with zero mean and standard deviation  $\sigma$ . The value of  $\sigma$  to be used depends on the

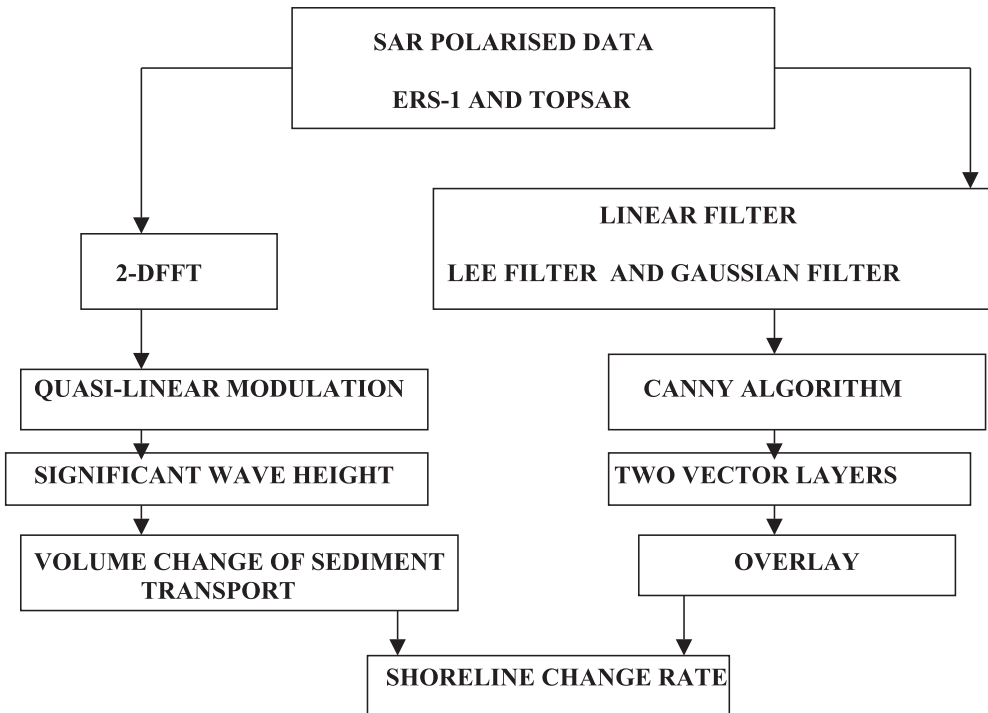


**Fig. 1:** Operational Model of Shoreline Change.

length of interesting connected contours, the noise level, and the localization-detection trade off. The Gaussian filtering was applied and smoothens the image intensity to image  $J$  i.e.,  $J = I * G$ . For each pixel  $(j, j)$ : (a) compute the gradient components,  $J_x$  and  $J_y$ , (b) estimate the edge strength as given by

$$e_s(i, j) = \sqrt{j_x^2(i, j) + j_y^2(i, j)} \quad (1)$$

and (c) estimates the orientation of the edge normal as given by

$$e_o(i, j) = \arctan \frac{j_y}{j_x} \quad (2)$$

The output is a strength image,  $E_s$ , formed by the values  $e_s(i, j)$  and an orientation image,  $E_o$  formed by the values  $e_o(i, j)$ . The shoreline edge pixels will be vectorized automatically after Canny algorithm has been performed. Canny algorithm was performed to two SAR polarized images in order to identify the rate of shoreline change.

## 2.4 Wave Spectra effects and Shoreline Changes

Wave spectra are derived from polarized SAR data by applying quasi-linear modulation transfer function (MTF). According to VACHON et al. (1994). The quasi-linear modulation transfer function (MTF) is adequate to describe the relationship between observed SAR image spectrum  $S(k)$  and the directional heave spectrum  $\psi(k)$ . The ground wave condition are collected from the Petronas oil platform at  $5^\circ 02' N$  and  $105^\circ 23' E$ . The wave spectra derived from polarized SAR data were mapped into the real wave spectra by using a forward quasi-linear model. This model was simplified by VACHON et al. (1994) as follows

$$S_q(k) = H(k_x; K_c) \left\{ |T_{lin}(k)|^2 \frac{\psi(k)}{2} + |T_{lin}(-K)|^2 \frac{\psi(-k)}{2} \right\} \quad (3)$$

where  $k_x$  is the azimuth wave-number component, and  $T_{lin}(k)$  is the linear MTF. The

azimuth cut-off function depends upon the cut-off azimuth wave-number by

$$H(k_x) = e^{\left(-\pi \frac{k_x^2}{k_c^2}\right)} \quad (4)$$

According to BEAL et al. (1983) an azimuthal cut-off wavelength  $\lambda_c$  in SAR image spectra of ocean waves that depends on significant wave height  $H_s$  and  $\frac{R}{V}$  through

$$\lambda_c \propto \left(\frac{R}{V}\right) \sqrt{H_s} \quad (5)$$

For fully developed wind seas with  $H_s < 1$  m which corresponds to wind speed less than 7 m/s. This dependence can be explained by low-pass azimuthal filter whose width is determined by the scene coherence time.

### 2.4.1 Significant Wave Height Model from SAR Data

In order to estimate the significant wave height from the quasi-linear transform VACHON et al. (1994) introduced the following formula:

$$L_c = (R/V) \sqrt{4.4 H_s + 0.13 U^2} \quad (6)$$

$H_s$  and  $U^2$  are the ground truth data of significant wave height and wind speed along the coastal waters of Malaysia. The measured wind speed was estimated for 10 m height above the sea surface. A least squares fit was used to find degree of correlation between cut-off wavelength, from equation (5), and the one calculated directly from the TOPSAR image. Then, the following equation was used to estimate  $H_s$  from the SAR image

$$L_c = 2.8 \left(\frac{R}{V}\right) \sqrt{H_s} \quad (7)$$

(VACHON et al. 1994), where  $R/V$  is the scene range-to-platform velocity ratio. For the TOPSAR  $R/V$  is approximately 32s.

## 2.5 Wave Refraction Plot

The wave refraction has been done by applying the Huygens' method. The Huygens' method was used to draw the refraction pattern rays as described in MAGED (2000). Huygens' method states that all points on the wave front can be considered as point sources for the production of spherical secondary wavelets. The new wave front is the envelope of all small wavelets.

Consider a fix point for wave propagation what are often termed spherical „Huygens' wavelets“ where the emergent wavelength is  $\xi(x,y)ds$  (Fig. 2). We let these spherical Huygens' wavelets emanating from all  $ds$  of the entire aperture propagate out to the point  $P(x,y)$  where the net effect is obtained by principle of superposition, i.e., by summing the reshaping of wave as it passes through different bottom topography. The amplitude of spherical Huygens' wavelets must decrease with distance  $1/r$ . From each point  $ds$  of the wave propagation there will be received at point  $P(x,y)$  a wave contribution which we shall call the differential  $dE$ :

$$dE = \frac{\xi(x,y)ds}{r} \cos(\omega t - kr) \quad (8)$$

## 2.6 Shoreline Change Model

The shoreline change model is based on the volumetric change of sediment transport. This mathematical model depends on the available input of breaker wave height and

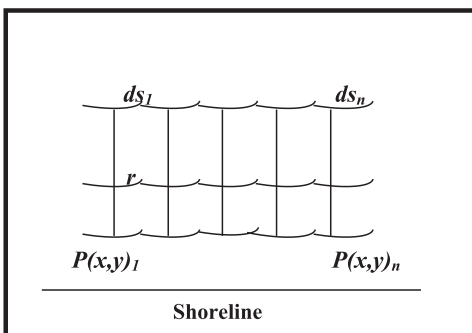


**Fig. 2:** Sketch of Huygens' Wavelets Concept.

direction of deepwater wave height. The longshore transport rate,  $Q$ , is the volumetric rate of the movement of the sand parallel to the shoreline.  $Q$  is expressed in the terms of sediment transport per unit volume (such as cubic meters per month). The method used to calculate the longshore transport is based on the assumption that longshore transport rate,  $Q$ , only dependent upon the longshore component of wave energy flux entering the surf zone.

The significant wave height determined by using quasi-linear and velocity bunching model is used to determine the depth of wave breaking. This can be given by

$$H_{sb} = 0.39 g^{1/5} (TH_s^2)^{2/5} \quad (9)$$

(KOMAR 1976).

This equation used to determine the depth of the breaking wave  $h$  as

$$\gamma_b = \frac{H_b}{h} \quad (10)$$

According to KOMAR (1976) the longshore sediment transport volume rate,  $Q$ , is calculated as

$$Q = 1.1 \rho g^{3/2} H_{bs}^{5/2} \sin \alpha_b \cos \alpha_b \quad (11)$$

where  $\rho = 1020 \text{ kg/m}^3$  for the sea water,  $g$  is  $9.8 \text{ m/s}^2$  and  $\alpha_b$  is the breaking wave angle.

In many cases, where the short-term shoreline change caused by cross-shore transport are small compared to the long-term changes, the one-line model is believed to identify the shoreline evolution. Following the assumption that the bottom profile moves in parallel to itself out of the depth of closure. The mass conservation of sand along an infinitely small length,  $dx$ , of the shoreline can be formulated as

$$\frac{\partial y}{\partial t} + D^{-1} \frac{\partial Q}{\partial x} = 0 \quad (12)$$

where  $y$  is the shoreline position ( $m$ ),  $x$  is the longshore coordinate ( $m$ ),  $t$  is the period (month),  $D$  is the depth of closure ( $m$ ), and  $Q$  is the longshore sand transport rate. In order to solve equation (12) the expressions

for the one quantity  $D$  must be formulated. HANSON (1989) introduced the following formula which given the annual depth of closure as slightly more than twice the maximum annual significant wave height ( $H_{mas}$ ). This can given as

$$D = 2 H_{mas} \tag{13}$$

This model was working with spatial resolution of 2 km over the shoreline of Kuala Terengganu. The window size of applying two dimension Fourier Transform was  $512 \times 512$  pixels. Each pixel represents a  $10\text{ m} \times 10\text{ m}$  area for TOPSAR and  $12.5\text{ m} \times 12.5\text{ m}$  for ERS-1. The entire image frame of TOPSAR and ERS-1 correspond to a  $5.12\text{ km} \times 5.12\text{ km}$  and a  $6.4\text{ km} \times 6.4\text{ km}$  patch on the ocean surface. This means that the wave spectra pattern extracted from  $6.4\text{ km} \times 6.4\text{ km}$  will show effect on sediment transport on equal area with 2 km along over the shoreline.

### 3 Results and Discussion

Canny algorithm can provide an automatic digitizing for shoreline (Fig. 3). The vector layers extracted by the implementation of Canny algorithm are observed in polarised SAR images. The coincided vector layers of ERS-1 and TOPSAR data shown a pronounce change (Fig. 4). It is obvious that the vector layers are digitized manually coincide with the vector layers extracted by the use of Canny algorithms (Fig. 5). This explains that the Canny algorithm provides edge detection for shorelines as possible as close to the true. It is obvious that the Canny algorithm can detect the concave shoreline. This is clearly demonstrated along the coastline of Sultan Mohamed Airport, as this area tends to be concave. This is because of the fact that the Canny algorithm produces pixel wide skeleton curves. Then a sequence of pixels along the curve was extracted from the two images. In addition, the sequence of pixels for each curve is converted to a vector pattern by fitting piecewise line segments to it. This induced polyline was an approximation to the original pixel curve.

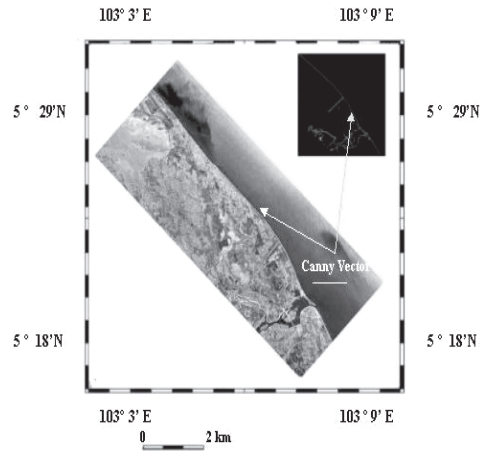


Fig. 3: Result of Canny Algorithm.

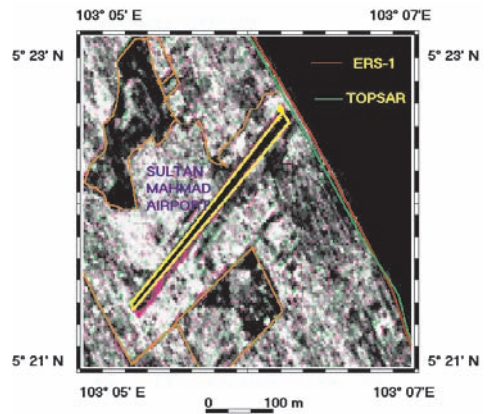


Fig. 4: Vector Layers Extracted by Canny Algorithm.

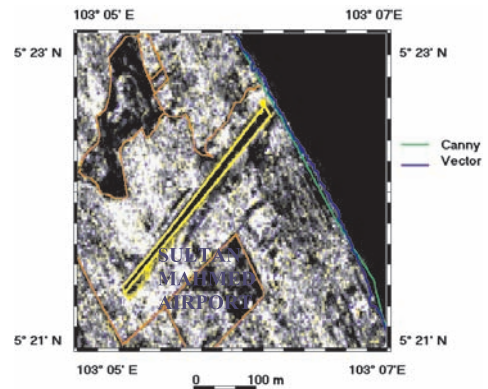


Fig. 5: Vector Layers of Canny Algorithm and Digitizing.

This could be attributed to the fact that the Canny algorithm links pairs of polylines. Therefore it would be easier to detect the concave shoreline feature (Fig 5). The rate of shoreline change is finally determined by overlaying the two vector layers from different periods that were extracted by using the Canny algorithm. It is also obvious that either *L* band or *C* band show good potential for shoreline detection.

The wave spectra among December 1996 and August 1993 show pronounce variation. It is obvious that the wavelength spectra are variable between August 1993 and December 1996 (Tab. 1).

**Tab. 1:** Ocean Wavelength Extracted from SAR Polarized data.

Sensor Type	Ocean Wavelength
ERS-1 (August 1993)	25 m–100 m
TOPSAR (December 1996)	20 m–170 m

It is obvious that the wave spectra propagated from northeast direction during December with wave length ranged between 20 to 170 m. In August, the wave spectra propagated from southeast direction with wavelength ranged between 25–100 m. It is obvious that the spectra peaks are shifted to the azimuth direction (Fig. 6). This could be attributed to the velocity bunching effects on SAR images. Fig. 7 shows the energy spectra derived by quasi-linear transform. The spectra peak of TOPSAR data is sharper with narrow band compared to ERS-1 data. This explained that wave spectra during December are more propagated in azimuth direction. As the waves are induced by the northeast monsoon seasons. This could be attributed to that azimuth cut-off is proportional directly with the significant wave height and wind speed. The significant wave height is proportional with the square root of wave energy. The largest wave spectra energy will be more concerted on azimuth direction (Fig. 7a). The lowest wave spectra energy are more symmetry along range and azimuth directions (Fig. 7b). This

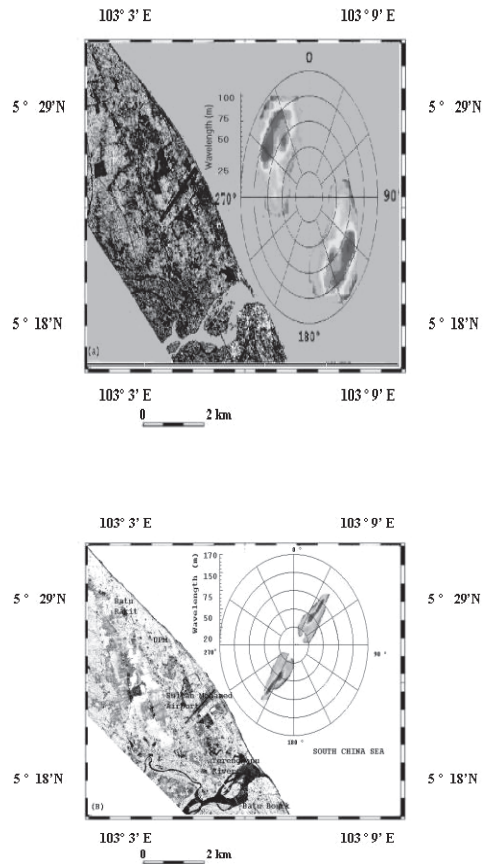


**Fig. 6:** Wave Spectra Derived from (a) ERS-1 and (b) TOPSAR Data, Respectively.

is obvious in August. August is the end of southwest monsoon season, the winds are started to change their directions from southeast to northeast directions. In this case wave spectra energy shown with lowest value with wide band. This could be caused the wave spectra peaks to be shifted between range and azimuth directions.

Fig. 8 shows the wave refraction pattern derived from ERS-1 and TOPSAR data. It is obvious that the wave rays during August 1993 and December 1996 converged on the shoreline of Sultan Mahamad Airport. This means that either the south or north wave propagations always converge on the shoreline of Sultan Mohamad Airport. It may be because the concave shape of the shoreline.

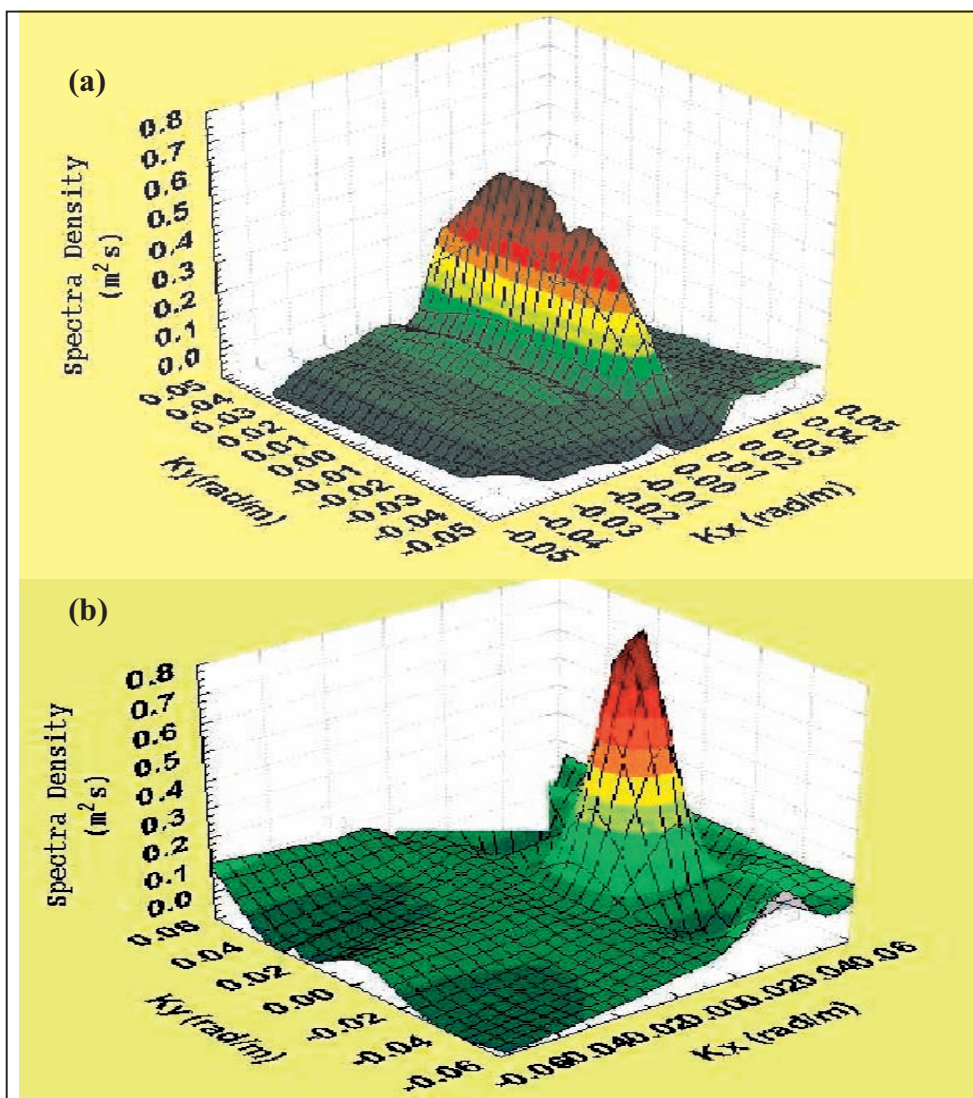


Fig. 7: Spectral Energy of (a) ERS-1 and (b) TOPSAR Data Derived from Quasi-linear Model.

The significant wave height was then used to model the change in sediment volume transport, in order to detect shoreline change. Fig. 9 shows that the rate of shoreline change peaks that have been modeled with the Canny algorithm coincide with the results from the quasi-linear model and the vector data (August 1993 and December 1996). It is obvious that there is a significant relation between the rate of shoreline change

that was modeled with the Canny algorithm and the volume of change of the sediment transport (Fig. 9).

The statistical significant t-test shows that a rate of significant difference is noticed between volume change of sediment transport and vector data obtained by manual digitizing. The rate of significant difference decreased with the ones that were automatically extracted by using the Canny algorithm



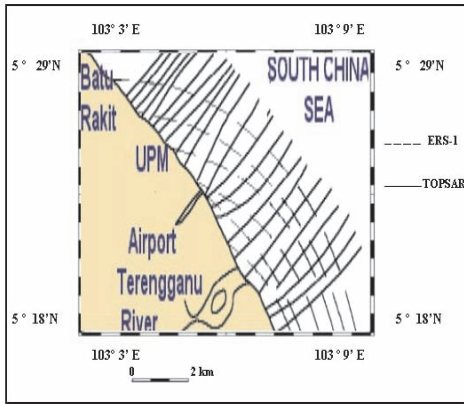


**Fig. 8:** Wave Refraction Derived by Huygen's Principle from ERS-1 and TOPSAR data.

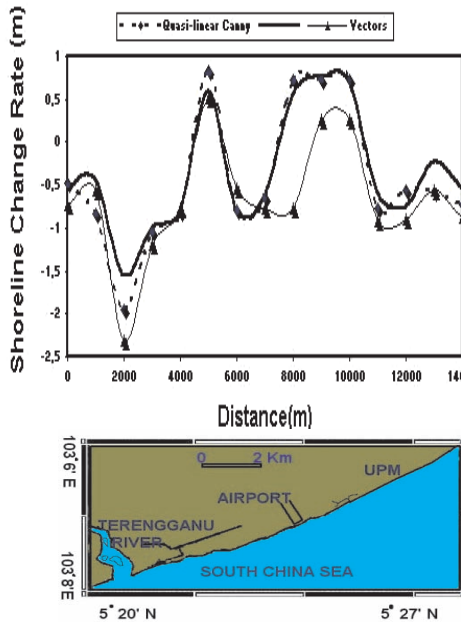


**Fig. 9:** Rate of Shoreline Change Derived from Canny, Quasi-linear Model and Digitizing Method.

and volume change of the sediment transport model. This could be attributed to some of the errors introduced by manual digitizing. This error could be the reason for the low accuracy rate. However, all the methods agreed on a high rate of erosion along the Sultan Mahmad Airport coastline of less than 1 m/year. This result is similar to the result of MAGED (1999) and MAGED (2000). However, this study does not agree with the study of MAZLAN et al. (1989). This is because of the fact that MAZLAN et al. (1989) defined the shoreline as the zone of high tide. This definition is not valid because of the fact that the tidal zone is a dynamic area in which the tide change its cycle between low and high tide. This could not be used as a basic reference for the shoreline.

#### 4 Conclusions

The Canny algorithm can be used for automatic detection of shoreline change from remotely sensed data. Operational use of remote sensing for an assessment of coastal erosion could be done by the application of wave spectra effects on volume change of sediment transport directly from radar data. This method should be integrated with automatic detection of shoreline change by using the Canny algorithm. The dominant erosion event along the shoreline of Sultan Mahmad Airport due to the concave shape of the shoreline. This induces a dominant wave convergence during the northeast monsoon and southeast monsoon seasons. It can be said that the SAR data good be used as tool for modeling shoreline change. This is because of the fact that SAR data able to model the roughness of sea surface compared to other optical and it be possible to model the shoreline change.

**Tab. 2:** Significan Differences T-test of Canny Algorithm with Quasi-linear and Vectors Layers.

Model Type	DF	Ts	T	Differences	p	Significant
Quasi-linear	20	1.45	1.2	0.2	0.13	non-sig.
Vector layers	20	2.32	3.2	0.0003	0.0002	Sig.

## References

- BAUER, E., HASSELMANN, K., YOUNG, I.R. & HASSELMANN, S., 1996: Assimilation of Wave Data into Wave Model AM Using an Impulse Response Function Method. – *J. Geophys. Res.* **101**: 3801–3816.
- EL-RAEY, M., NASR, S.M. & EL-HATTAB, M.M., 1995: Change Detection of Rosetta promontory over the Last Forty Years. – *Int. J. Remote Sensing* **16** (5): 825–834.
- FRIGHY, O.E., NASR, S.M., EL HATAB, M.M. & EL RAEY, M., 1995: Remote sensing of Beach Erosion Along the Rosetta Promontory, Northwestern Nile Delta, Egypt. – *Int. J. Remote Sensing* **15** (8): 1649–1660.
- HANSON, H., 1989: Genesis – A Generalised Shoreline Change Numerical Model. – *Journal of Coastal Research* **5**: 1 – 27.
- KOMAR, P.D., 1976: Beach Processes and Sedimentation. – Prentice-Hall, New Jersey.
- LUKMAN, M.H., ROSNAN, Y. & SAAD, S., 1995: Beach Erosion Variability during a North-east Monsoon: The Kuala Setiu Coastline, Terengganu, Malaysia. – *J. Pertanika* **3** (2): 337–348.
- MAGED, M.M., 1994: Coastal Water Circulation of Kuala Terengganu. – M.Sc. Thesis, Universiti Pertanian Malaysia.
- MAGED, M.M., 1999: Predication of Coastal Erosion by Using Radar Data. – Proceedings of IGARSS' 99. Hamburg, Germany.
- MAGED, M.M., 2000: Wave Spectra Studies and Shoreline Change by Remote Sensing. – Ph. D. Thesis, Universiti Putra Malaysia.
- MAZLAN, H., AZIZ, I. & ABDULLAH, A., 1989: Preliminary Evaluation of Photogrammetric-Remote sensing Approach in Monitoring Shoreline Erosion. – Proceeding of the Tenth Asian Conference on Remote Sensing. November 23–29, 1989. Kuala Lumpur, Malaysia, pp: F-5-1 – F-5-10.
- RAJ, J.K., 1982: Net Directions and Rates of Present-day Beach Sediment Transport by Littoral Drift along the East Coast of Peninsular Malaysia. – *Geol. Soc., Malaysia Bull.* **15**: 57–82.
- VACHON, P.W., HAROLD, K.E. & SCOTT, J., 1994: Airborne and Spaceborne Synthetic Aperture Radar Observations of Ocean Waves. – *J. Atmo.-Ocean* **32** (10): 83–112.

Address of the author:  
 Dr. MAGED MARGHANY  
 Faculty of Science and Technology  
 Department of Marine Science  
 College University Science and Technology  
 21030 Kuala Terengganu, Malaysia  
 e-mail: magedupm@hotmail.com

Manuskript eingegangen: März 2001  
 Angenommen: Mai 2001